Rapid fragmentation during seeded lysozyme aggregation revealed at the single molecule level

Kubankova, Marketa; Lin, Xiaoyan; Albrecht, Tim; Edel, Joshua B; Kuimova, Marina K

DOI:
10.1021/acs.analchem.9b01221

Document Version
Peer reviewed version

Citation for published version (Harvard):
Kubankova, M, Lin, X, Albrecht, T, Edel, JB & Kuimova, MK 2019, 'Rapid fragmentation during seeded lysozyme aggregation revealed at the single molecule level', *Analytical Chemistry*, vol. 91, no. 10, pp. 6880-6886. https://doi.org/10.1021/acs.analchem.9b01221

Rapid fragmentation during seeded lysozyme aggregation revealed at the single molecule level

Markéta Kubánková[1†], Xiaoyan Lin[1†], Tim Albrecht[1,2]*, Joshua B. Edel[1]*, Marina K. Kuimova[1]*

[1] Department of Chemistry, Imperial College London, Exhibition Road, London SW7 2AZ, UK

[2] School of Chemistry, Edgbaston Campus, University of Birmingham, Birmingham B15 2TT, UK

† M. K. and X. L. contributed equally to this work.

*Corresponding authors; correspondence to m.kuimova@imperial.ac.uk, joshua.edel@imperial.ac.uk, t.albrecht@imperial.ac.uk.

Protein aggregation is associated with neurodegenerative disorders such as Alzheimer's and Parkinson's diseases. The poorly understood pathogenic mechanism of amyloid diseases makes early-stage diagnostics or therapeutic intervention a challenge. Seeded polymerisation that reduces the duration of the lag phase and accelerates fibril growth is a widespread model to study amyloid formation. Seeding effects are hypothesised to be important in the 'infectivity' of amyloids and are linked to the development of systemic amyloidosis in vivo. The exact mechanism of seeding is unclear yet critical to illuminating the propagation of amyloids. Here we report on the lateral and axial fragmentation of seed fibrils in the presence of lysozyme monomers at short timescales, followed by the generation of oligomers and growth of fibrils. These results may form the basis for future studies of therapeutic intervention.

Peptides and proteins have the propensity to convert from their soluble forms into highly organised aggregates called amyloids, fibrillar quaternary structures ordered into β-sheets, rich in intermolecular hydrogen bonds.[1] Amyloids are associated with diseases such as Alzheimer's and Parkinson's. Nevertheless, amyloid materials are now also known to have important functional roles in organisms.[2-3]

Protein aggregation is a complex multi-pathway process and the precise mechanism of amyloid assembly is specific for each protein, but there are common characteristics for all amyloids.[4] Certain types of intermediates are typically formed on the way to amyloid fibrils, some of which are able to spread and cause nucleation elsewhere.[5-7] It is believed that small intermediates are the most cytotoxic species and that they are highly related to the propagation of amyloids.[8-12] Such species are usually short-lived, and their presence at low concentration could be masked in bulk measurements based on ensemble average.[6, 13-14] The mechanism of how these species are generated, how they propagate and catalyse further formation of aggregates is still poorly understood.

A typical aggregation pathway occurs as follows (Figure 1a): under certain conditions, a monomeric protein misfolds and starts assembling with other monomers to form oligomers. These small soluble oligomers act as nuclei for the formation of larger species - protofibrils and mature fibrils; this process is called primary nucleation. In the next stage, the protofibrils and fibrils grow and elongate, but this may also be accompanied by a degree of fragmentation.[6] Fragmentation of fibrils is believed to be one of the most critical propagation pathways for amyloid fibrils.[6-7, 11, 14-19] Previous studies have revealed that mature fibrils can break into small intermediates, which provide additional growth surface and enhance toxicity.[11, 14, 20] The study of such microscopic processes not only elucidates the pathogenic mechanism, but also provides potential targets for therapeutic intervention.[21]

To date there is no direct evidence that amyloids are infectious in the same manner as prions, but an increasing number of studies contend that the pathogenesis of amyloidosis is carried out through templated corruption of particular amyloidogenic proteins.[22] For this reason, seeded polymerisation is an important model for studying protein aggregation. It is well established that amyloid fibril formation from monomeric proteins is greatly enhanced by the introduction of preformed 'seed' fibrils.[23-24] Seeding effects appear to be important in the 'infectivity' of amyloids, similar to prion transmission, and are linked to the development of systemic amyloidosis *in vivo*.[23-25] Studies of seeded aggregation have focused mainly on the effect of seeding on the kinetics of fibril formation *in vitro*, *e.g.* reporting the disappearance of a slow lag phase corresponding to primary nucleation.[26] However, the mechanism of seed intervention is still unclear with no mechanistic studies reported to date.

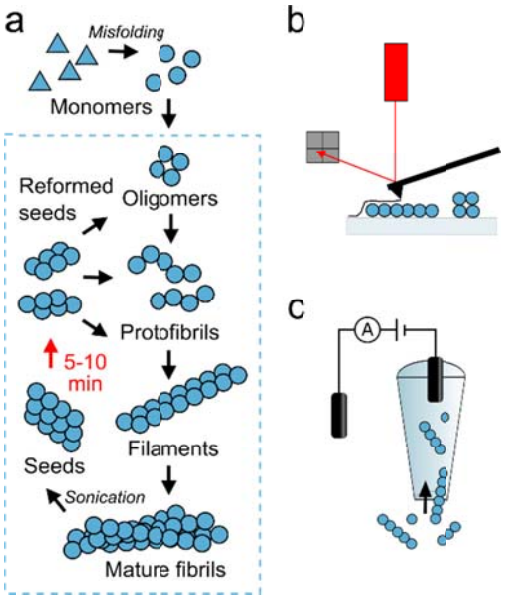

Figure 1. Schematic diagram of seeded aggregation of lysozyme and the two single molecule detection methods employed in this study. **(a)** Proposed mechanism of the disassembly of seeds and its effect on the formation of amyloid fibrils. **(b)** Principle of imaging protein aggregates via atomic force microscopy. **(c)** Working principle of the nanopore-based single molecule sensing.

The use of single molecule detection methods could represent a step towards a better understanding of protein aggregation and the effects of seeding, offering a distinct advantage of being able to monitor individual molecules in a complex and heterogeneous population. Such techniques are potentially able to reveal rare events, *e.g.* small oligomeric intermediates or seeds present at 1%, masked in more conventional bulk measurements. In this work, atomic force microscopy (AFM)[20, 27] (Figure 1b) and nanopore sensing[28-33] (Figure 1c) were employed to elucidate the pathway of seeded aggregation of lysozyme, a protein connected to systemic amyloidosis and commonly used as an *in vitro* model system for amyloid assembly,[34] at the single molecule level.

AFM is a powerful tool for imaging the structural properties and topology of surface-immobilised biological samples, such as proteins and DNA.[35-38] Accordingly, AFM has been widely employed for studying the morphology of different species of amyloids[39-41]. In conjunction with suitable immobilisation strategies (so that the surface species accurately reflect the solution conditions),[42-43] it can also be used to study the solution composition and its temporal evolution, on time scales from minutes to many hours. With this in mind, we here utilise AFM in order to directly characterise the dimensions of species formed during lysozyme aggregation and for quantitative determination of the interconversion between species.

On the other hand, nanopore sensing is a single-molecule method that does not rely on surface immobilisation of species and as such is ideally suited for providing information about the aggregation process in solution. In a typical nanopore experiment, charged molecules are driven through a nanopore ('translocate') by an externally applied electric field, resulting in a temporal modulation of the measured ionic current, which reflects the size and charge of translocating species.[28, 32-33, 44] Previously, nanopore sensing has been used to

study the aggregation pathway of α-synuclein, lysozyme and β–amyloid.[29, 31, 33]

In our experiments, aliquots were periodically taken out of aggregating solution, diluted and examined by these two modalities of single molecule detection: AFM reporting on the changing morphology of species over the course of aggregation; electrical measurements through nanopores, sensitive to size and charge of translocating species.

Together these two methods provide important new insight into the complex and dynamic process of seeded lysozyme aggregation and reveal new features and timescales of crucial stages of this process. Most notably, both lateral and axial fragmentation of lysozyme seed fibrils was observed at a short time scale not previously considered possible, followed by the formation of small species capable of propagation.

Results

The disassembly and reassembly of seed fibrils studied via atomic force microscopy

The unique advantage of AFM lies in the high-resolution structural detail in 3D and the ability to noninvasively detect individual biomolecules through the tapping mode, in which the probe tip oscillates and gently taps the sample surface. In our experiments, aliquots were extracted from the aggregating protein solution at different time points of incubation, diluted, applied to freshly cleaved mica and dried. We note that in our analysis we make the assumption that the distributions of species are representative of the solution composition, *i. e.* that immobilisation is comparable for all species in solution.

In our study we were particularly interested in processes occurring directly after seeding. In freshly seeded samples (T = 0 min), AFM revealed the presence of relatively thick short fibrils (Figures 2a, b), often organised in clusters. The diameter of these species (determined as the height) had a broad distribution with a peak value of 2.4 ± 0.9 nm (Figure 2b), similar to the distribution in a pure seed sample (Figure S1). Lysozyme monomers could not be detected directly by AFM under the conditions used here. Within the first 5 minutes of incubation, the height decreased, Figure 2b, as the seed fibrils laterally disassembled into thin rigid fibrils with mean thickness of 1.3 ± 0.1 nm (Figure S2), from here on referred to as filaments. In addition to the decreasing height, we noted a significant decrease in contour length of the species during the first 10 minutes (Figure 2c). From qualitative analysis of the AFM images it appears that seeds tend to fragment at junctions between individual rigid sections and disassemble into basic units of 50-100 nm in length (Figure S3). At T = 15 min, the prevalence of filament fibrils remained, but the appearance of thicker species (not exceeding 3 nm) is clear from the histogram. Moreover, the sample had a significantly higher proportion of species with 100-200 nm contour length, compared to T = 0 min and T = 5 min. Between 5 and 15 minutes of incubation there is a decrease of contour length, largely due to the sudden appearance of small spherical oligomers (Figure S4c), but simultaneously there is evidence for increasing height (Figure S5). After T = 15 min there was a clear increase of contour lengths and a broader distribution of lengths (Figure S6).

To confirm that the unexpected disassembly of seeds was caused by the addition of monomers, rather than by the change in temperature and pH during sample preparation, control experiments were carried out with sonicated seeds, but without monomers, at the same buffer conditions and temperature. Without the addition of monomers (Figure S7), neither fragmentation or fibril growth was observed even after 60 minutes, with little change in the contour length and thickness. These results verified the monomer-assisted secondary nucleation during the aggregation process.

At T = 60 min, the concentration of elongated fibrils increased, often including branch formation, which was reflected in the increasing population of long contour lengths (Figure 2c). We also observed significant broadening of the height distribution, as a heterogeneous population of thick fibrils was formed (Figure 2b). Further thickening and elongation of fibrils was evident at later time points, and the fibrils became highly branched and intertwined (Figure S4e). These results were complemented with nanopore measurements, as detailed below. In control experiments, where the monomeric lysozyme solution was not seeded, only small non-fibrillar species were observed at T = 30 min and T = 60 min (Figure S8). The absence of long fibrils at this time point in non-seeded experiments demonstrates a significantly slower growth rate compared to seeded protein aggregation, where long fibrils started to appear within the first hour of sample incubation (Figure 2a).

Over the course of aggregation, the thinnest observed unit with filamentous organisation were flexible aggregates with an apparent mean height of 0.6 ± 0.2 nm (Figure 2d), from here on referred to as protofibrils. The length of these species was extremely short, not exceeding 200 nm (Figure S2). In contrast to rigid segments of mature fibrils (Figure S9), the protofibrils did not have straight segments; they had flexible and coiling structure. A large population of protofibrils was present even at T = 42 h alongside thick mature fibrils.

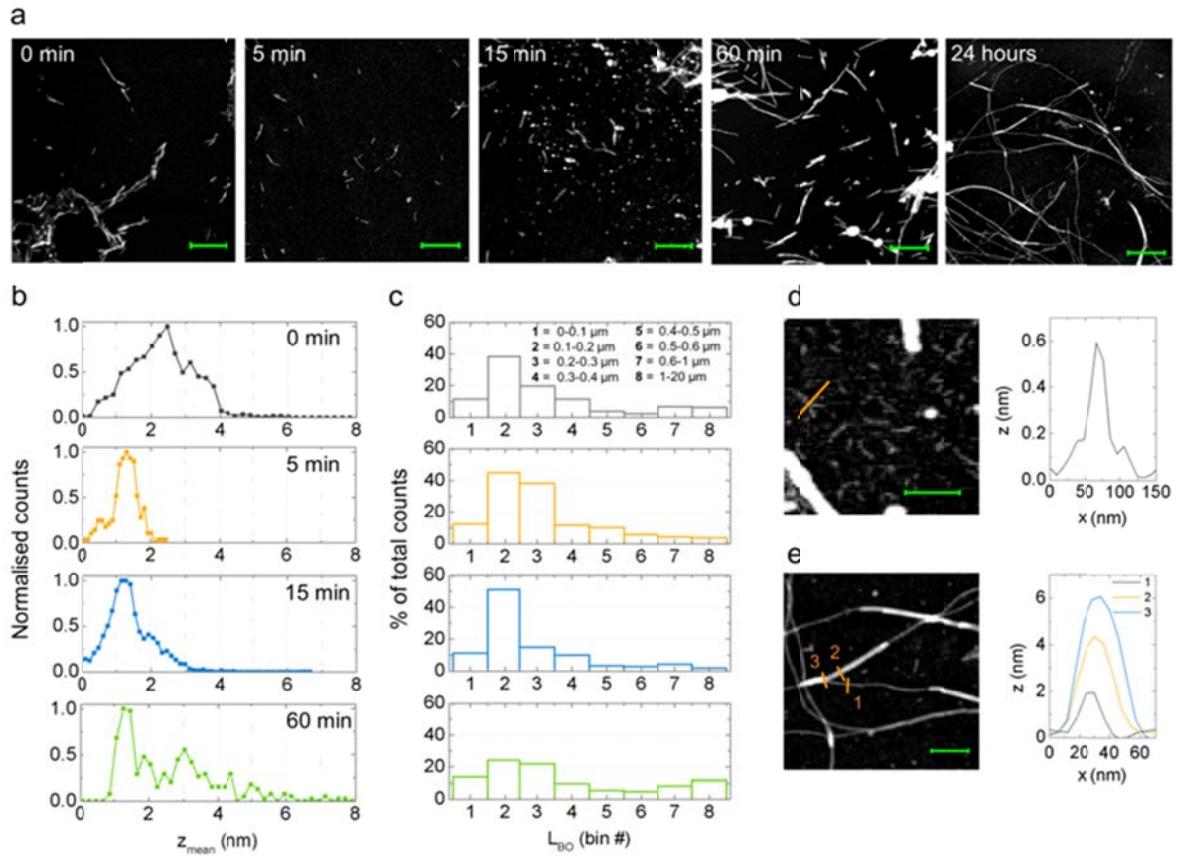

Figure 2. Atomic force microscopy of lysozyme aggregates. **(a)** Atomic force microscopy images at 0 min, 5 min, 15 min, 60 min and 24 h of seeded lysozyme aggregation in solution. Scale bars = 500 nm. **(b)** Height distributions of species in 0 min, 5 min, 15 min, 60 min samples; protofibrils (0.6 nm height) were excluded from the analysis at 15 and 60 min due to their unchanging large proportion. **(c)** Distributions of contour lengths of species in these samples (non-linear binning, see legend for details). The number of molecules used for calculating each sample distribution ranged between 180 – 760. **(d)** The smallest observed filamentous species, flexible protofibrils, with a mean height z = 0.6 nm, and the z-profile corresponding to the section marked in orange. Scale bar = 200 nm. **(e)** Detail of the 24 h image demonstrating a junction of fibrils with corresponding z-profiles of the 3 sections marked on the image. Scale bar = 200 nm.

Filaments and mature rigid fibrils were observed to have heights in multiples of 0.6 nm, suggesting that protofibrils may be an intermediate to fibril formation. Both odd and even multiples of 0.6 nm were observed, suggesting that protofibril units may add on laterally to form thicker species (Figure 2e, Figure S2). Linear elongation was observed as well. Moreover, periodic height patterns in images (Figure S10) confirmed that mature fibrils can twist together, forming thicker fibrils with height approximately corresponding to the sum of the constituent fibrils (Figure 2e). It is important to note that the heights within single branched filaments were very heterogeneous, especially at late time points, which is evident from the detail of the 24 h sample in Figure 2e, showing 1.8nm-, 4.2nm- and 6nm-thick fibrils. The thickest observed late stage fibril was 12 nm in height (data not shown).

Characterising the aggregation process by nanopore sensing

Although AFM revealed the lateral and axial fragmentation of seed fibrils in the presence of monomers at short time scales, we wanted to see whether these findings could be

supported by a solution-based single-molecule method, such as nanopore sensing. The latter does not rely on surface immobilisation and should provide complementary information about the aggregation process in solution.

In a typical nanopore experiment, charged molecules translocate through a nanopore due to an externally applied electric field. The resulting temporal modulation of the measured ionic current reflects on the size and charge of translocating species.[28, 32-33, 44]

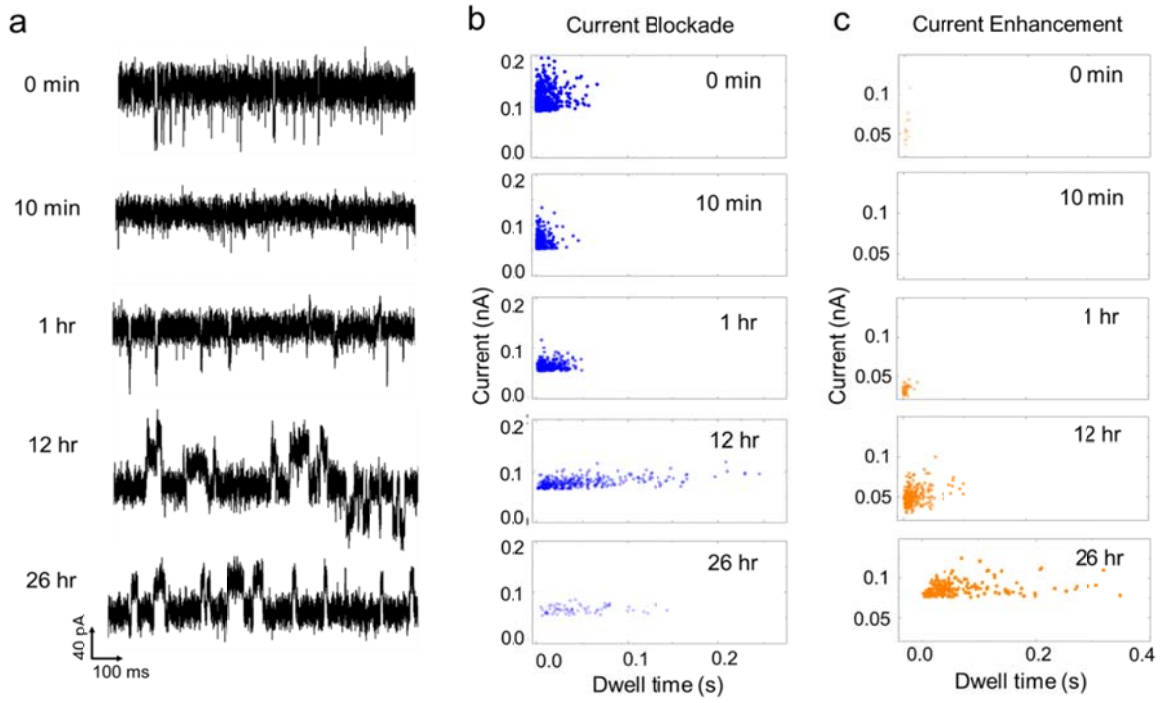

Figure 3. Current – time traces of lysozyme aggregates at 0 min, 10 min, 1 h, 12 h and 26 h after seeding. The translocation was conducted in buffer containing 10 mM Tris, 1 mM EDTA, 100 mM KCl, pH 7.4. 2 - 4 µL of each sample collected at different time points of aggregation was added to a reservoir for the single molecule translocation studies. All the current traces were recorded at an applied voltage of 600 mV. **(b, c)** The heat plots of current versus dwell time at various aggregation time points for current blockade (**b**) and current enhancement (**c**) events.

Nanopore translocation experiments for different stages of lysozyme aggregation were performed in 100 mM KCl using quartz capillaries with a 30 nm nanopore opening (from here on referred to as nanopores, Figure S11). The nanopore was functionalised with polybrene to minimize the protein-pore interaction and avoid blockage (Figure S12). Two parameters were recorded: (1) dwell time, the duration of the time that the protein molecules spend in the nanopore; (2) current modulation, the amplitude of the current change during the translocation of molecules. Current – time traces at 0 min, 10 min, 1 h, 12 h and 26 h are shown in Figure 3. The median dwell times of events with current blockade and current enhancement are shown in Figure 4a,b, respectively, together with the current/dwell time distributions in Figure 3b,c. At time T = 0 min, current blockades were observed with dwell

times up to ca 20 ms. Fragmentation of the seeds was clearly observed over the first 10 minutes, with dwell times and current blockades decreasing by 61% and 43%, respectively. This correlates well with the AFM data, indicative of seed fragmentation **(**in thickness and in length).

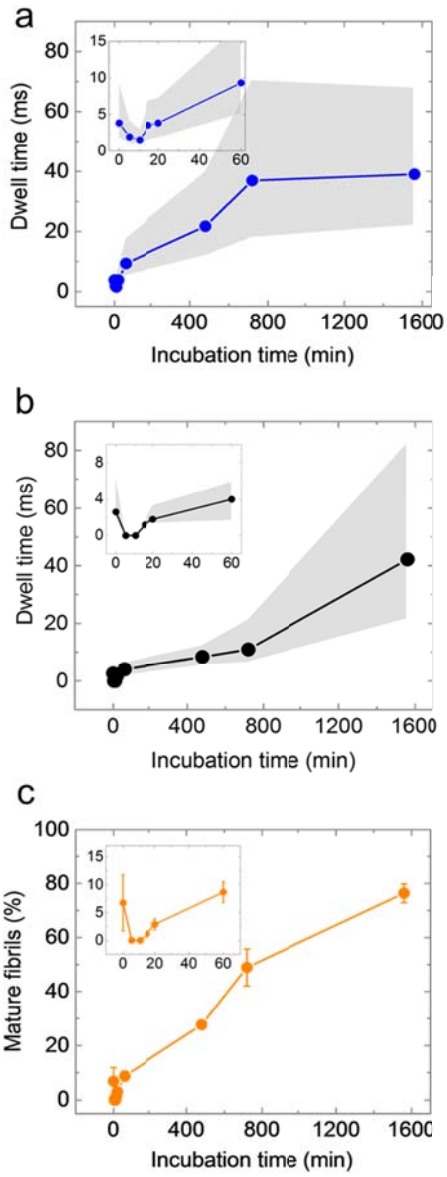

Figure 4. The median dwell time of lysozyme aggregates in the nanopore with current blockade **(a)** and current enhancement **(b)** at various time points of sample incubation; the grey shadowed area indicates 25% to 75% confidence zone. **(c)** The proportion of mature fibrils detected as the ratio of current enhancement events to total events, at various aggregation time points.

After 15 minutes, the dwell times of events with current blockade and current enhancement started to rise (Figure 4a,b), reflecting the gradual elongation of filaments and fibrils. Moreover, with increasing incubation time, the dwell time distribution broadened (Figure 3b,c, Figure 4a,b). Specifically at T = 60 min, the dwell time distribution broadened by 130% compared to T=15 min. This correlated with the increasing dispersity of aggregates measured by AFM, namely the distribution of contour lengths, which at T = 60 min broadened by

260% compared to T = 15 min (Figure S6). Importantly, as incubation time increased, the number of events with current blockade decreased in the nanopore experiments, and the number of events with current enhancement increased (Figure 3b,c). Translocation events with current enhancement (rather than blockade) became dominant at late time points, as can be seen in Figure 3b,c and Figure 4c, the latter shows the ratio of the number of events exhibiting current enhancement to total events is plotted. The median dwell time of the events with current enhancement (Figure 4b) showed similar trend as that of the events with current blockade (Figure 4a).

We attributed the current enhancement to mature fibrils, with an increase in current being caused by differences of the surface charge due to the twisting of two or more filaments and displacement of charged amino acid side chains from the surface. During nanopore translocation, the biomolecule displaces the ions inside the pore, which results in a decrease of the current (current blockade). However, due to accumulation of counterions shielding the biomolecule in the nanopore, it is also possible to have current enhancement. In this work, the accumulation of negative counterions on the surface of the twisted fibrils may contribute to the increased conductance and to the current enhancement,[45-46] which is consistent with zeta potential measurements (Figure S13) and charge distribution calculated from the nanopore data (Figure S14). We note that to rule out the effect of pH changes on the observed charge variation, we confirmed that the pH of the solution is stable during the aggregation process (data not shown). The proportion of mature fibrils decreased from 7% at 0 min to 0% at 5 min and 10 min, increased again to 1% at 15 min, 49% at 12 h and 76% at 26 h (Figure 4c).

Discussion

One of the most important insights that the combination of two single-molecule methods has revealed in this study was the fragmentation of seed fibrils on a short timescale, at least in the *in vitro* experiments. Previously, fluorescence lifetime detection of an environmentally sensitive fluorophore (a so called molecular rotor) $DiSC_2(3)$ using conventional confocal microscopy has revealed unexpected reduction in microscopic viscosity in the early stages of the seeded aggregation of lysozyme.[47] However, in this study that used fluorescence detection from the 'bulk' of the sample, the mechanistic details behind the reduction of viscosity were not possible to identify. In our present experiments at the single molecule level, within the first 10 minutes of seeded aggregation of lysozyme, axial and lateral disassembly of seeds was reported by AFM and nanopore measurements. We account the initial decrease of height and length to monomer-assisted fragmentation of seed fibrils, linked with secondary nucleation. Our hypothesis is supported by a combination of facts. Between 0 to 5 minutes, the shortening of linear species was apparent from AFM images and histograms, as well as from the nanopore dwell time. At 5-10 minutes of incubation, upwards events with current enhancement, assigned to mature fibrils, completely disappeared from nanopore measurements. The disassembly of seeds was also apparent from the AFM data. Our experiments demonstrated that neither fragmentation nor secondary nucleation happen in the absence of lysozyme monomers under the studied conditions.

A large number of oligomeric species was detected by AFM at T = 15 min following seeding. We performed incubation experiments in which either (1) lysozyme monomers were present and seed fibrils were absent, or (2) seed fibrils were present and monomers were absent; neither of these cases resulted in an upsurge of oligomers at T = 15 min. Thus, we hypothesise that the oligomers observed under the 'standard' incubation conditions were generated via secondary nucleation, which was induced by the disassembly of seed fibrils into thin short filaments. Previous research has shown that the twisted thick mature fibril cannot serve as a lateral binding site for monomers.[20] We believe that the disassembly of seed fibrils provides binding sites for monomers, leading to secondary nucleation. These processes lead to a large number of fibril fragments and oligomers, species known to be easily diffusible and highly cytotoxic,[7, 25] implicating deleterious effects in disease.

Studies of fibril fragmentation have found that fragmentation rates are dependent on the length and concentration of seed fibrils, the solution pH, temperature and agitation.[9, 48] In the conditions of our experiments the fragmenting seed fibrils were relatively short, yet the fragmentation occurred on a strikingly short time scale not observed by other researchers.[6, 11, 14-15] Prior to our work, compared to fibril elongation rates, fragmentation rates are considered to be slow.[49]

In addition to fibrils and oligomers, we observed short flexible protofibrils with previously unreported extremely small mean height of ca 0.6 nm; likely formed by stacking addition of monomeric or oligomeric units.[50] The observed height is below the size expected for lysozyme,[39, 51] as the monomeric dimensions of lysozyme are 3·3·4.5 nm[52] and the smallest filamentous aggregate reported in literature had a height of 2 nm.[39, 41, 51] We cannot tell with certainty at this stage whether the small dimensions of protofibrils detected by AFM reflect the true state in solution, or are affected by protein-surface/probe-surface interactions or are the result of the clustering of lysozyme monomers on the mica surface.[42] While the observation of extremely thin protofibrils is intriguing, according to literature, they are not capable of acting as seeds[40] and thus are not likely to play roles in propagation of disease.

For the assembly of filaments and mature fibrils, AFM and nanopore data suggest that small lysozyme species can add on axially or laterally through various pathways: a) axial elongation through the addition of monomeric, oligomeric or protofibril units), b) lateral addition of monomers onto filaments, which results in branching and secondary nucleation, c) lateral stacking of two protofibrils or lateral addition of a protofibril to existing filaments, d) twisting of filaments into mature fibrils[40] and twisting between mature fibrils, as sensed by current enhancement events in the nanopore sensing.

During the growth phase, lysozyme fibrils undergo a remarkable change of surface charge, as reported by nanopore and zeta potential measurements. Since the electrostatics of the protein depends on the accessibility of amino acids that can ionise, the change of surface charge possibly results from charged amino acid side chains becoming buried during the lateral growth and twisting of lysozyme fibrils.

Conclusions

We present evidence that upon seeding of a monomeric lysozyme solution with fibril fragments, the seeds undergo structural reforming on short time scales that were not considered previously. We collect mechanistic and structural data on the role of the seeding process in the formation of oligomers, which may be an important stage in spreading of the disease *in vivo*. We reveal the details of changes to structure, charge and packing of lysozyme, during the process of aggregation. Since it is believed that the replication and propagation of amyloids *in vivo* may occur through the seeding-nucleation pathway, these new insights on seeded protein aggregation could be an important element in understanding the mechanism of spreading of amyloids during diseases, which may form the basis for future biomedical studies of therapeutic intervention in amyloid diseases.

Methods

Lysozyme aggregation preparation. Hen egg white lysozyme (HEWL, 14307 Da, 129 amino acids, product code L6786) and all solvents (spectroscopic grade) were purchased from Sigma-Aldrich. The protein was left to defrost for 5 minutes at room temperature. 1 mL of fresh solution of HEWL was prepared in a glass vial at 4 mg/mL with 50 mM HCl, 100 mM NaCl, first letting the protein dissolve in 50 mM HCl solution, gently shaking and consequently adding salt. The monomer solution was passed through a syringe driven filter of 0.22 μm pore size. The solution was seeded with 1 % v/v sonicated preformed fibrils and allowed to aggregate at 57°C. The seeds were prepared by incubating a solution of 60 mg/mL HEWL in 50 mM HCl, 200 mM NaCl at 60°C for 12 hours and subsequent sonication to obtain short seed fibrils. Higher salt concentration (200 mM vs 100 mM) was used to accelerate fibril formation [47]. The relatively low temperature of 57-60°C for aggregation reactions was intentionally chosen in order to minimize the formation of amorphous aggregates. [53]

Atomic force microscopy. Aliquots from the aggregating protein solution were diluted 200 or 400 times with filtered water; 2 μL of this mixture was applied to freshly cleaved mica (Agar Scientific) and incubated at room temperature for 5 min. Images were obtained in tapping mode in air at room temperature from at least three independently prepared samples using an Agilent Technologies 5500 and 9500 AFM/SPM microscopes and commercial "Super Sharp Silicon" AFM probes (Windsor Scientific). To prevent artefacts from tip wear, each image was acquired using a new tip at 0.1-0.2 lines/s with 512 × 512 pixels and scan areas of 5 × 5 μm^2. Images were processed in Gwyddion software with a third order "flatten filter", grains were marked using watershed segmentation.

Nanopore fabrication and functionalisation. The quartz capillaries (Intracel Ltd, UK) exhibit an outer diameter of 1.0 mm and an inner diameter of 0.5 mm including inner filament. After being cleaned in the plasma cleaner, the capillaries were pulled by a laser-based pipette puller (Sutter Instrument, P-2000) through a two-line protocol: (1) HEAT, 575; FIL, 3; VEL, 35; DEL, 145; PUL, 75; (2) HEAT, 700; FIL, 0; VEL, 15; DEL, 128; PUL, 200. It should be noted that the parameters are instrument specific, and were optimized to yield a nanopore of approximately 30 nm. The functionalisation of the nanopore was obtained by immersing the capillaries (both inside and outside) in a 7.5% polybrene solution for 15 min and subsequently rinsing them with the translocation buffer. Newly functionalised nanopores were used for each time point.

Single molecule detection with nanopore. The translocation buffer contains 10 mM Tris, 1 mM EDTA, 100 mM KCl, pH 7.4; 2-4 μL of each sample collected at different time points of aggregation was added to a reservoir for the single molecule translocation studies. All the current traces were recorded at an applied voltage of 600 mV. For translocation experiments, electrodes (Ag/AgCl) were inserted into the external bath (patch electrode) and the capillary (ground electrode), respectively. The ion currents of protein translocations through the nanopore were measured with AxoPatch 200B patch clamp amplifier (Molecular Devices, US), filtered with a 10 kHz Bessel filter and recorded by the software pClamp 10 (Molecular Devices). The data was analysed using a custom-written MATLAB code.

Zeta potential measurement. 2 μL of the sample was diluted in 1 mL H_2O and the zeta potential was determined using a Zetasizer Nano (Malvern Instruments Ltd.). All measurements were repeated at least three times.

Data availability. The datasets generated during and analysed during the current study are available from the corresponding author on request.

Acknowledgements

M. K. K. is thankful to the EPSRC for the Career Acceleration Fellowship (EP/I003983/1). J. B. E. has been funded in part by an ERC starting and consolidator investigator grants. X. L. and M. K. were funded by Imperial College President's Scholarship.

Author contributions

M. K. K., J. B. E. and M. K. conceived the experiments, M. K. K., J. B. E. and T. A. designed the experiments. X. L. and M. K. performed the experiments: M. K. performed AFM characterisation, X. L. conducted nanopore sensing. X. L., M. K. and J. B. E. analysed the data. M. K., X. L., M. K. K., T. A. and J. B. E. co-wrote the paper. As X. L. and M. K contributed equally to this work, author order was decided via probabilistic methods. All authors reviewed the manuscript.

Additional information

Competing financial interests: The authors declare no competing financial interests.

References

1. Dobson, C. M., Protein misfolding, evolution and disease. *Trends Biochem. Sci.* **1999,** *24* (9), 329-332.
2. Ross, C. A.; Poirier, M. A., Protein aggregation and neurodegenerative disease. *Nat. Med.* **2004,** *10* (7), S10-S17.
3. Knowles, T. P. J.; Vendruscolo, M.; Dobson, C. M., The amyloid state and its association with protein misfolding diseases. *Nat. Rev. Mol. Cell Biol.* **2014,** *15* (6), 384-396.
4. Chiti, F.; Dobson, C. M., Protein misfolding, functional amyloid, and human disease. *Annu. Rev. Biochem.* **2006,** *75*, 333-66.
5. Jucker, M.; Walker, L. C., Self-propagation of pathogenic protein aggregates in neurodegenerative diseases. *Nature* **2013,** *501* (7465), 45-51.
6. Cohen, S. I. A.; Linse, S.; Luheshi, L. M.; Hellstrand, E.; White, D. A.; Rajah, L.; Otzen, D. E.; Vendruscolo, M.; Dobson, C. M.; Knowles, T. P. J., Proliferation of amyloid-beta 42 aggregates occurs through a secondary nucleation mechanism. *Proc. Natl. Acad. Sci. USA* **2013,** *110* (24), 9758-9763.
7. Schnabel, J., AMYLOID Little proteins, big clues. *Nature* **2011,** *475* (7355), S12-S14.
8. Haass, C.; Selkoe, D. J., Soluble protein oligomers in neurodegeneration: lessons from the Alzheimer's amyloid beta-peptide. *Nat. Rev. Mol. Cell Biol.* **2007,** *8* (2), 101-12.
9. Buell, A. K.; Galvagnion, C.; Gaspar, R.; Sparr, E.; Vendruscolo, M.; Knowles, T. P. J.; Linse, S.; Dobson, C. M., Solution conditions determine the relative importance of nucleation and growth processes in alpha-synuclein aggregation. *Proc. Natl. Acad. Sci. USA* **2014,** *111* (21), 7671-7676.

10. Harper, J. D.; Lansbury, P. T., Models of amyloid seeding in Alzheimier's disease and scrapie: Mechanistic truths and physiological consequences of the time-dependent solubility of amyloid proteins. *Annu. Rev. Biochem.* **1997,** *66*, 385-407.
11. Knowles, T. P. J.; Waudby, C. A.; Devlin, G. L.; Cohen, S. I. A.; Aguzzi, A.; Vendruscolo, M.; Terentjev, E. M.; Welland, M. E.; Dobson, C. M., An Analytical Solution to the Kinetics of Breakable Filament Assembly. *Science* **2009,** *326* (5959), 1533-1537.
12. Soto, C.; Estrada, L.; Castilla, J., Amyloids, prions and the inherent infectious nature of misfolded protein aggregates. *Trends Biochem. Sci.* **2006,** *31* (3), 150-155.
13. Shammas, S. L.; Garcia, G. A.; Kumar, S.; Kjaergaard, M.; Horrocks, M. H.; Shivji, N.; Mandelkow, E.; Knowles, T. P. J.; Mandelkow, E.; Klenerman, D., A mechanistic model of tau amyloid aggregation based on direct observation of oligomers. *Nat. Commun.* **2015,** *6*, 1-10.
14. Arosio, P.; Knowles, T. P. J.; Linse, S., On the lag phase in amyloid fibril formation. *Phys. Chem. Chem. Phys.* **2015,** *17* (12), 7606-7618.
15. Cohen, S. I. A.; Vendruscolo, M.; Dobson, C. M.; Knowles, T. P. J., From Macroscopic Measurements to Microscopic Mechanisms of Protein Aggregation. *J. Mol. Biol.* **2012,** *421* (2-3), 160-171.
16. Ruschak, A. M.; Miranker, A. D., Fiber-dependent amyloid formation as catalysis of an existing reaction pathway. *Proc. Natl. Acad. Sci. USA* **2007,** *104* (30), 12341-12346.
17. Ferrone, F., Analysis of protein aggregation kinetics. *Method Enzymol* **1999,** *309*, 256-274.
18. Xue, W. F.; Homans, S. W.; Radford, S. E., Systematic analysis of nucleation-dependent polymerization reveals new insights into the mechanism of amyloid self-assembly. *P Natl Acad Sci USA* **2008,** *105* (26), 8926-8931.
19. Tornquist, M.; Michaels, T. C. T.; Sanagavarapu, K.; Yang, X.; Meisl, G.; Cohen, S. I. A.; Knowles, T. P. J.; Linse, S., Secondary nucleation in amyloid formation. *Chem Commun (Camb)* **2018**.
20. Jeong, J. S.; Ansaloni, A.; Mezzenga, R.; Lashuel, H. A.; Dietler, G., Novel Mechanistic Insight into the Molecular Basis of Amyloid Polymorphism and Secondary Nucleation during Amyloid Formation. *J. Mol. Biol.* **2013,** *425* (10), 1765-1781.
21. Arosio, P.; Vendruscolo, M.; Dobson, C. M.; Knowles, T. P. J., Chemical kinetics for drug discovery to combat protein aggregation diseases. *Trends Pharmacol. Sci.* **2014,** *35* (3), 127-135.
22. Walker, L. C.; Diamond, M. I.; Duff, K. E.; Hyman, B. T., Mechanisms of Protein Seeding in Neurodegenerative Diseases. *JAMA neurology* **2013,** *70* (3), 10.1001/jamaneurol.2013.1453.
23. Come, J. H.; Fraser, P. E.; Lansbury, P. T., Jr., A kinetic model for amyloid formation in the prion diseases: importance of seeding. *Proc. Natl. Acad. Sci. USA* **1993,** *90* (13), 5959-63.
24. Jarrett, J. T.; Lansbury, P. T., Jr., Seeding "one-dimensional crystallization" of amyloid: a pathogenic mechanism in Alzheimer's disease and scrapie? *Cell* **1993,** *73* (6), 1055-8.
25. Xue, W. F.; Hellewell, A. L.; Gosal, W. S.; Homans, S. W.; Hewitt, E. W.; Radford, S. E., Fibril fragmentation enhances amyloid cytotoxicity. *J. Biol. Chem.* **2009,** *284* (49), 34272-82.
26. Krebs, M. R.; Wilkins, D. K.; Chung, E. W.; Pitkeathly, M. C.; Chamberlain, A. K.; Zurdo, J.; Robinson, C. V.; Dobson, C. M., Formation and seeding of amyloid fibrils from wild-type hen lysozyme and a peptide fragment from the beta-domain. *J. Mol. Biol.* **2000,** *300* (3), 541-9.
27. Neuman, K. C.; Nagy, A., Single-molecule force spectroscopy: optical tweezers, magnetic tweezers and atomic force microscopy. *Nat. Methods* **2008,** *5* (6), 491-505.
28. Howorka, S.; Siwy, Z., Nanopore analytics: sensing of single molecules. *Chem. Soc. Rev.* **2009,** *38* (8), 2360-84.

29. Hu, R.; Diao, J. J.; Li, J.; Tang, Z. P.; Li, X. Q.; Leitz, J.; Long, J. G.; Liu, J. K.; Yu, D. P.; Zhao, Q., Intrinsic and membrane-facilitated alpha-synuclein oligomerization revealed by label-free detection through solid-state nanopores. *Sci. Rep.* **2016,** *6*, 1-11.
30. Ivanov, A. P.; Actis, P.; Jonsson, P.; Klenerman, D.; Korchev, Y.; Edel, J. B., On-Demand Delivery of Single DNA Molecules Using Nanopipets. *Acs Nano* **2015,** *9* (4), 3587-3595.
31. Martyushenko, N.; Bell, N. A. W.; Lamboll, R. D.; Keyser, U. F., Nanopore analysis of amyloid fibrils formed by lysozyme aggregation. *Analyst* **2015,** *140* (14), 4882-4886.
32. Miles, B. N.; Ivanov, A. P.; Wilson, K. A.; Dogan, F.; Japrung, D.; Edel, J. B., Single molecule sensing with solid-state nanopores: novel materials, methods, and applications. *Chem. Soc. Rev.* **2013,** *42* (1), 15-28.
33. Yusko, E. C.; Prangkio, P.; Sept, D.; Rollings, R. C.; Li, J. L.; Mayer, M., Single-Particle Characterization of A beta Oligomers in Solution. *Acs Nano* **2012,** *6* (7), 5909-5919.
34. Pepys, M. B.; Hawkins, P. N.; Booth, D. R.; Vigushin, D. M.; Tennent, G. A.; Soutar, A. K.; Totty, N.; Nguyen, O.; Blake, C. C. F.; Terry, C. J.; et al., Human lysozyme gene mutations cause hereditary systemic amyloidosis. *Nature* **1993,** *362* (6420), 553-7.
35. Kaminski Schierle, G. S.; van de Linde, S.; Erdelyi, M.; Esbjorner, E. K.; Klein, T.; Rees, E.; Bertoncini, C. W.; Dobson, C. M.; Sauer, M.; Kaminski, C. F., In situ measurements of the formation and morphology of intracellular beta-amyloid fibrils by super-resolution fluorescence imaging. *J. Am. Chem. Soc.* **2011,** *133* (33), 12902-5.
36. Pinotsi, D.; Buell, A. K.; Galvagnion, C.; Dobson, C. M.; Kaminski Schierle, G. S.; Kaminski, C. F., Direct observation of heterogeneous amyloid fibril growth kinetics via two-color super-resolution microscopy. *Nano Lett.* **2014,** *14* (1), 339-45.
37. Japrung, D.; Bahrami, A.; Nadzeyka, A.; Peto, L.; Bauerdick, S.; Edel, J. B.; Albrecht, T., SSB binding to single-stranded DNA probed using solid-state nanopore sensors. *J. Phys. Chem. B* **2014,** *118* (40), 11605-12.
38. Nuttall, P.; Lee, K.; Ciccarella, P.; Carminati, M.; Ferrari, G.; Kim, K. B.; Albrecht, T., Single-Molecule Studies of Unlabeled Full-Length p53 Protein Binding to DNA. *J. Phys. Chem. B* **2016,** *120* (9), 2106-14.
39. Arnaudov, L. N.; de Vries, R., Thermally induced fibrillar aggregation of hen egg white lysozyme. *Biophys. J.* **2005,** *88* (1), 515-26.
40. Harper, J. D.; Lieber, C. M.; Lansbury, P. T., Jr., Atomic force microscopic imaging of seeded fibril formation and fibril branching by the Alzheimer's disease amyloid-beta protein. *Chem. Biol.* **1997,** *4* (12), 951-9.
41. Chamberlain, A. K.; MacPhee, C. E.; Zurdo, J.; Morozova-Roche, L. A.; Hill, H. A.; Dobson, C. M.; Davis, J. J., Ultrastructural organization of amyloid fibrils by atomic force microscopy. *Biophys. J.* **2000,** *79* (6), 3282-93.
42. Kim, D. T.; Blanch, H. W.; Radke, C. J., Direct imaging of lysozyme adsorption onto mica by atomic force microscopy. *Langmuir* **2002,** *18* (15), 5841-5850.
43. Rivetti, C.; Guthold, M.; Bustamante, C., Scanning force microscopy of DNA deposited onto mica: equilibration versus kinetic trapping studied by statistical polymer chain analysis. *J. Mol. Biol.* **1996,** *264* (5), 919-32.
44. Lin, X.; Ivanov, A. P.; Edel, J. B., Selective single molecule nanopore sensing of proteins using DNA aptamer-functionalised gold nanoparticles. *Chem. Sci.* **2017,** *8*, 3905-3912.
45. Smeets, R. M. M.; Keyser, U. F.; Krapf, D.; Wu, M. Y.; Dekker, N. H.; Dekker, C., Salt dependence of ion transport and DNA translocation through solid-state nanopores. *Nano Lett.* **2006,** *6* (1), 89-95.
46. Japrung, D.; Dogan, J.; Freedman, K.; Nadzeyka, A.; Bauerdick, S.; Albrecht, T.; Kim, M. J.; Jemth, P.; Edel, J. B., Single-Molecule Studies of Intrinsically Disordered Proteins Using Solid-State Nanopores. *Anal Chem* **2013,** *85* (4), 2449-2456.
47. Thompson, A. J.; Herling, T. W.; Kubankova, M.; Vysniauskas, A.; Knowles, T. P. J.; Kuimova, M. K., Molecular Rotors Provide Insights into Microscopic Structural Changes During Protein Aggregation. *J. Phys. Chem. B* **2015,** *119* (32), 10170-10179.

48. Hill, T. L., Length dependence of rate constants for end-to-end association and dissociation of equilibrium linear aggregates. *Biophys. J.* **1983,** *44* (2), 285-8.
49. Nakatani-Webster, E.; Nath, A., Inferring Mechanistic Parameters from Amyloid Formation Kinetics by Approximate Bayesian Computation. *Biophys J* **2017,** *112* (5), 868-880.
50. Hill, S. E.; Robinson, J.; Matthews, G.; Muschol, M., Amyloid protofibrils of lysozyme nucleate and grow via oligomer fusion. *Biophys. J.* **2009,** *96* (9), 3781-90.
51. Cao, A.; Hu, D.; Lai, L., Formation of amyloid fibrils from fully reduced hen egg white lysozyme. *Protein Sci.* **2004,** *13* (2), 319-24.
52. Blake, C. C. F.; Koenig, D. F.; Mair, G. A.; North, A. C. T.; Phillips, D. C.; Sarma, V. R., Structure of hen egg-white lysozyme. A three-dimensional Fourier synthesis at 2 Angstrom resolution. *Nature* **1965,** *206* (4986), 757-61.
53. Ow, S. Y.; Dunstan, D. E., The effect of concentration, temperature and stirring on hen egg white lysozyme amyloid formation. *Soft Matter* **2013,** *9* (40), 9692-701.